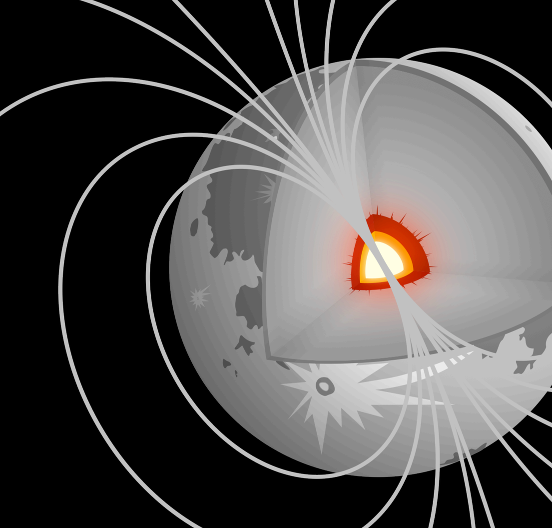

A Precession-Driven Lunar Dynamo Model

Bob Y. Tian[1a], Sabine Stanley[1b], Sonia M. Tikoo[2], Benjamin P. Weiss[3], Jack Wisdom[3]

1. Department of Physics, University of Toronto ([1a]ytian@physics.utoronto.ca, [1b]stanley@physics.utoronto.ca)
2. Department of Earth and Planetary Science, University of California Berkeley
3. Department of Earth, Atmospheric and Planetary Sciences, Massachusetts Institute of Technology

UNIVERSITY OF TORONTO

Introduction

There are several lines of evidence that a core dynamo once operated for the Moon. Orbital measurements of magnetic anomalies indicate a remanent magnetic field in large areas of the lunar crust [1]. In addition, paleomagnetic analyses of Apollo samples point towards a strong magnetic field with surface intensities of 10 – 110 μT operating between 4.25 and 3.56 billion years ago [2–5]. Furthermore, the paleointensities are observed to decrease to < 4μT between 3.56 and 3.19 billion years ago [6].

Cooling of crustal rocks in the presence of a steady magnetic field generated by a core dynamo is the only mechanism consistent with all lunar paleomagnetic studies [3–8]. A model of the lunar dynamo must be able to not only generate the observed longevity and paleofield strength at the surface, but also reproduce the timing of its rapid decline. The small size of the core and of the Moon itself is problematic for canonical convective dynamo models to replicate these features.

Alternative to convection, precessional energy was also readily available to drive the lunar dynamo earlier in the orbital evolution of the Earth-Moon system [9]. In this study, we solve the full magnetohydrodynamics (MHD) equations for a dynamo driven by differential precession of the core and the mantle.

Rotational States of the Core and Mantle

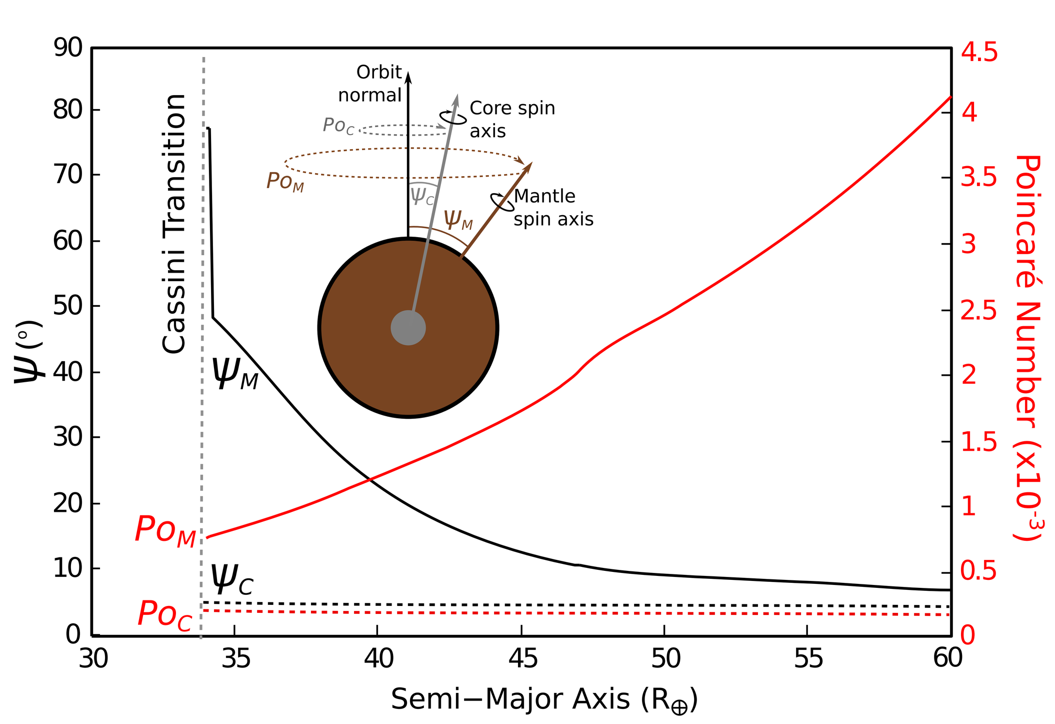

Figure 1. *Red Lines:* Poincaré number $Po = \alpha/\Omega_0$ (the ratio of precession frequency α and rotation frequency Ω_0) of the core [dashed line] and mantle [solid line] as a function of the lunar semi-major axis. Data for the mantle are taken from [11]. *Black Lines:* Obliquity of the lunar core [dashed line] and mantle [solid line] spin axis. Mantle obliquity from [10] axis receded beyond 26 - $29R_E$ [13].

The lunar spin axis is currently inclined 6.7° from the orbit normal, and precesses at a period of 18.6 years [10]. However, in the past, the obliquity M of the lunar spin axis may have been as high as 77° when the Moon first transitioned to its present Cassini state at an orbital distance of $34R_E$ from Earth [11].

Although the mantle precessed at frequencies depending on its obliquity, the core's precession was decoupled from the mantle sometime during the evolution of the lunar orbit. In the case of the Moon, the core is thought to be aligned with the ecliptic and precesses at a constant tilt about the orbit normal, as suggested by laser ranging experiments [12].

The evolution of the obliquity as a function of the semi-major axis a of the lunar orbit can be fit to a polynomial for a > $34.2R_E$ [9]:

$$\begin{aligned}\psi(x) = 0.1075x^{10} - 0.0332x^9 - 1.0008x^8 + 0.611x^7 \\ +2.7016x^6 - 1.7281x^5 - 2.328x^4 - 1.4509x^3 \\ +6.9951x^2 - 6.6208x + 10.7428\end{aligned} \qquad (1)$$

where $x = 0.1294(a/R_E - 46.308)$

As the Moon's semimajor axis increased further, the mantle obliquity eventually decreased towards present-day values of 6.7°. At some point during this decrease in obliquity, the mechanical power available to drive the core dynamo would also decrease below some critical value. Thus, this mechanical-dynamo model has the potential of reproducing both the longevity and decline of paleofield intensities. The evolution of the rotational states of the lunar core and mantle throughout its orbital evolution are summarized in Figure 1.

Model Equations & Parameters

We solve for the magnetic field **B** and velocity field **u** of the following system of nondimensional MHD equations in a precessing spherical shell with angular velocity $\boldsymbol{\Omega} = \boldsymbol{\Omega}_0 + \boldsymbol{\omega}$. Here, $\boldsymbol{\omega}$ is the perturbation to the rotation rate of the reference frame from the mean rotation rate $\boldsymbol{\Omega}_0$.

$$\nabla \cdot \mathbf{u} = 0 \qquad (2)$$

$$\nabla \cdot \mathbf{B} = 0 \qquad (3)$$

$$\begin{aligned} Ro_M\left(\frac{\partial}{\partial t} + \mathbf{u}\cdot\nabla\right)\mathbf{u} + 2\sin\psi_0\left(\sin(\alpha t)\hat{\boldsymbol{y}} - \cos(\alpha t)\hat{\boldsymbol{x}} + \frac{2-\cos\psi_0}{\sin\psi_0}\hat{\boldsymbol{z}}\right)\times\mathbf{u} \\ + \frac{Po}{2Ro_M}\sin\psi_0\left(\cos(\alpha t)\hat{\boldsymbol{y}} - \sin(\alpha t)\hat{\boldsymbol{x}}\right)\times\mathbf{r} = -\nabla p + (\nabla\times\mathbf{B})\times\mathbf{B} + E\nabla^2\mathbf{u}\end{aligned} \qquad (4)$$

$$\frac{\partial \mathbf{B}}{\partial t} = \nabla\times(\mathbf{u}\times\mathbf{B}) + \nabla^2\mathbf{B}. \qquad (5)$$

This non-dimensional form is controlled by the magnetic Rossby number Ro_M, the Ekman number E, and the Poincaré number Po. The variable α is the non-dimensionalized precession frequency of the reference frame. Values for the control parameters are given in Table 1. Free-slip boundaries were employed at the ICB. At the CMB, the flow field are forced towards the velocity of the differentially precessing mantle.

Parameter	Definition	Model Values	Lunar Values
inner-outer core radius ratio	$r_{io} = r_i/r_o$	0.5	0-0.7 *
Ekman number	$E = \nu/(2\Omega_0 r_o^2)$	$3\times10^{-6} - 5\times10^{-3}$	$3\times10^{-12} - 3\times10^{-11}$ *
magnetic Rossby number	$Ro_M = \eta/(2\Omega_0 r_o^2)$	$3\times10^{-6} - 5\times10^{-3}$	$3\times10^{-7} - 3\times10^{-6}$ *
Poincaré number of the mantle	$Po_M = \alpha_M/\Omega_0$	2.09×10^{-4}	2.09×10^{-4}
Poincaré number of the core	$Po_C = \alpha_C/\Omega_0$	$7.5\times10^{-4} - 2\times10^{-3}$	$7.5\times10^{-4} - 2\times10^{-3}$
obliquity of the mantle	ψ_M	$10° - 60°$	$10° - 60°$
obliquity of the core	ψ_C	$5.16°$	$5.16°$

Table 1. Control parameters for the dynamo models. r_i and r_o are the radii of the inner and outer core respectively, ν is the kinematic viscosity, Ω_0 is the mean rotation rate, and α_M and α_C are the precession rates of the mantle and the core respectively. (*) denotes ranges given due to uncertainty of current observations, rather than a range of values applicable to the Moon throughout its orbital history.

Model Outputs

Figure 2 is a snapshot of the solutions to one of the models, and displays a mostly dipolar field at the surface with an intensity of order 1μT.

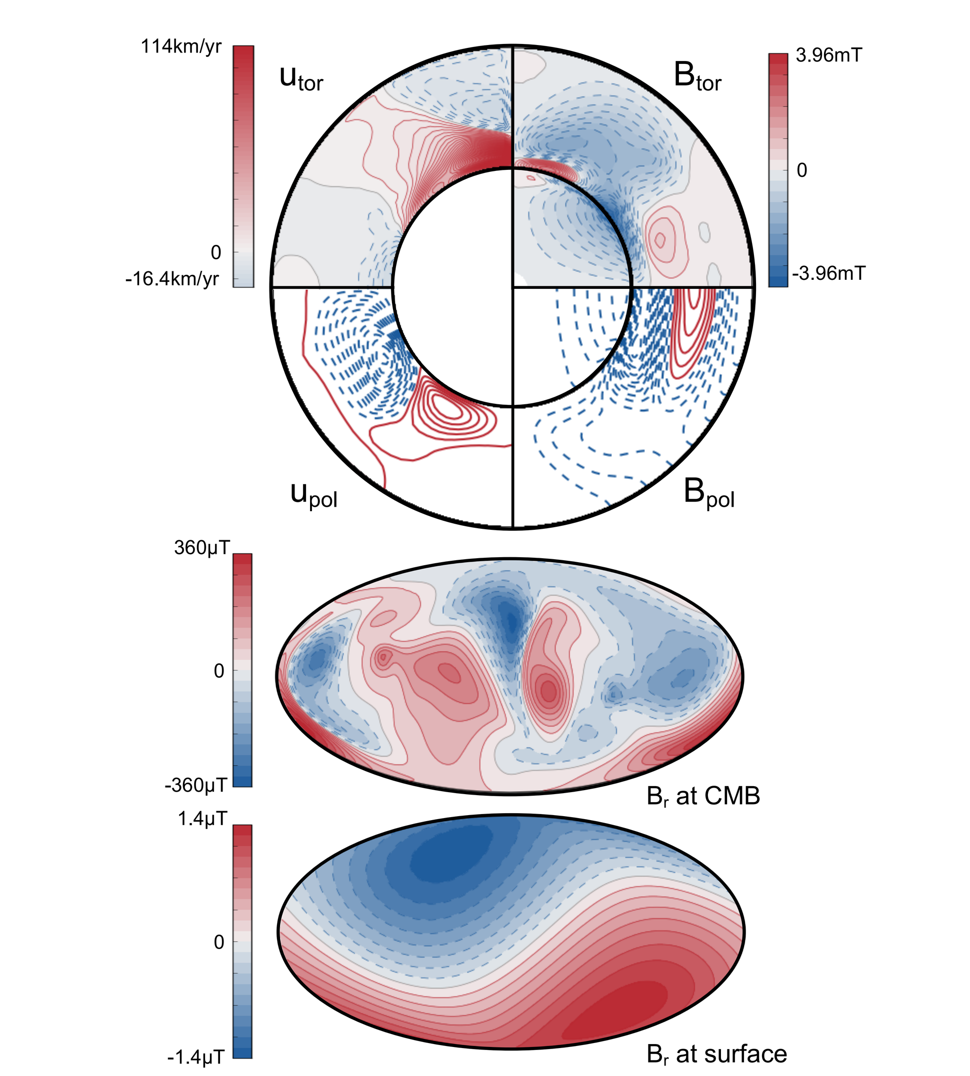

Figure 2. *Top:* axially averaged toroidal magnetic (B_{tor}) and velocity fields (u_{tor}), and poloidal streamlines of magnetic (B_{pol}) and velocity fields (u_{pol}). All axially averaged fields are symmetric about the equator, and thus only half of the field slices are shown. *Bottom:* Radial component of the magnetic field (B_r) plotted at the CMB and the surface. This model's parameters are: $\psi_M = 60°$, $Ro_M = E = 5\times10^{-5}$, and $Po_C = 7.5\times10^{-4}$

Critical Mantle Obliquities for Dynamo Action

In our mechanically driven dynamo model, the forcing is parameterized to scale with Ro_M^{-1}. It is too computationally expensive to use a lunar Ro_M in dynamo simulations. Thus, in order to infer properties of the lunar dynamo, we have carried out simulations over a range of magnetic Rossby number values for different obliquities. We find that a precessionally driven core in the lunar parameter regime is supercritical to dynamo action when the mantle obliquity is > 15°, and subcritical when the mantle obliquity is < 10°.

A summary of the parameter space explored in terms of Ro_M and ψ_M is plotted in Figure 3.

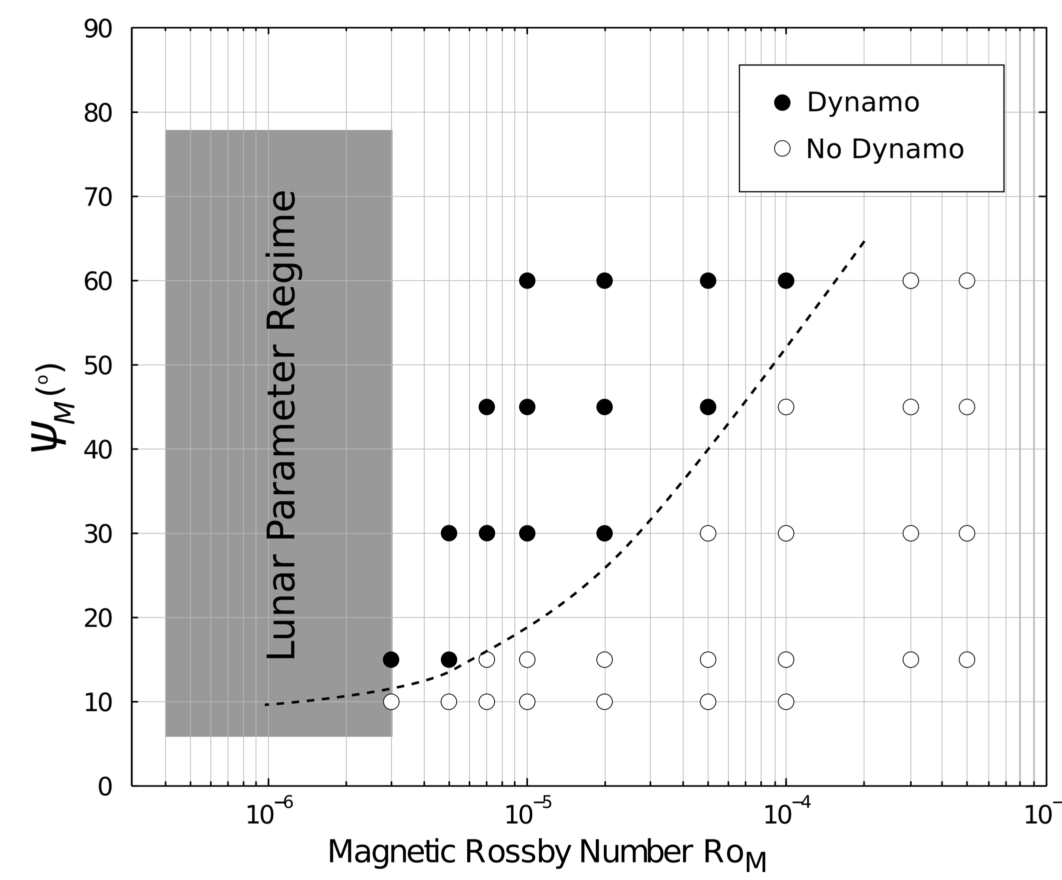

Figure 3. Summary of the parameter space explored. Filled dots indicate models in which the dynamo did not decay. To help guide the eyes of the readers, a dashed curve is drawn separating the two regions in the parameter space.

Surface Field Strength Scaling

We have also derived scaling laws for the surface field intensity as a function of Ro_M. We find that the surface intensity is stronger for lower Ro_M values. We also find that the surface intensity is higher at higher obliquities. Figure 4 demonstrates that the scaling laws we found predict lunar surface field intensities in the range of 1 – 100μT.

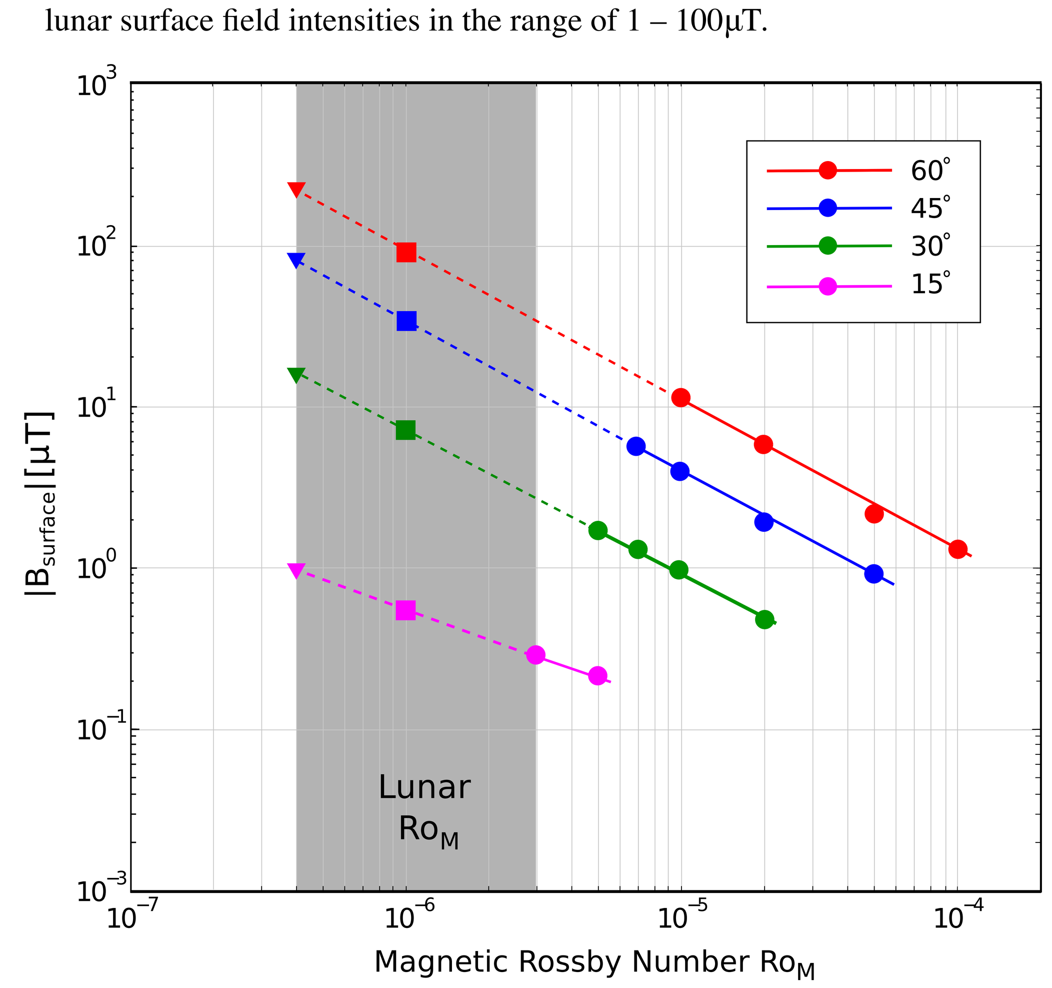

Figure 3. Surface magnetic field intensity vs. magnetic Rossby number for various mantle obliquities (each obliquity corresponds to a specific time in the Moon's orbital evolution). Dashed lines are drawn to extrapolate surface field intensity at lunar conditions of. The squares mark the predicted surface field intensity if the magnetic Rossby number of the Moon is 10^{-6}. The triangles are the predicted surface intensity if $Ro_M = 3\times10^{-7}$.

Paleointensities

Using the extrapolated surface field intensities for various obliquities in Figure 3, we can relate the magnetic field strength to Earth-Moon separation using the lunar orbital evolution model given in Figure 1. This is plotted in Figure 4 as paleointensity vs. semi-major axis.

To relate paleointensity generated by the models to the paleomagnetic record, we must constrain the timing of each mantle obliquity by converting semi-major axis a to time t. This is highly dependent on the orbital evolution model we use.

To illustrate the extreme uncertainty in converting semimajor axis into a time-axis, we plotted the paleomagnetic data from Apollo samples [3–6, 14] using the nominal a-to-t conversion in [9], which was a modified a-to-t relationship from models c and d of [15], and second time axis determined from the orbital evolution models from [16] (Fig. 4). Depending on the model, the Cassini state transition could have occurred anywhere between 4.2 Ga and 3.8 Ga, leading to a surge in surface magnetic field intensity. However, both models place the cessation of the lunar dynamo sometime after ~3.3 Ga and before ~2.7 Ga, consistent with the paleomagnetic record [6]. Furthermore, both a-to-t relationships lead to similar timing for the dynamo's rapid decline after 3.56 Ga, also consistent with results from [6].

Thus, our study demonstrates that the alternate possibility of a mechanically-driven lunar dynamo is capable of reproducing the lunar paleomagnetic record. Our model has the advantage of having mechanisms (i.e. core-mantle decoupling and differential precession) that are readily predicted to occur in lunar history [10-12, 17], and can explain two of the key perplexing features in the lunar paleomagnetic record: the longevity of the lunar dynamo, and the precipitous decline of surface intensities between 3.56 and 3.19 Ga.

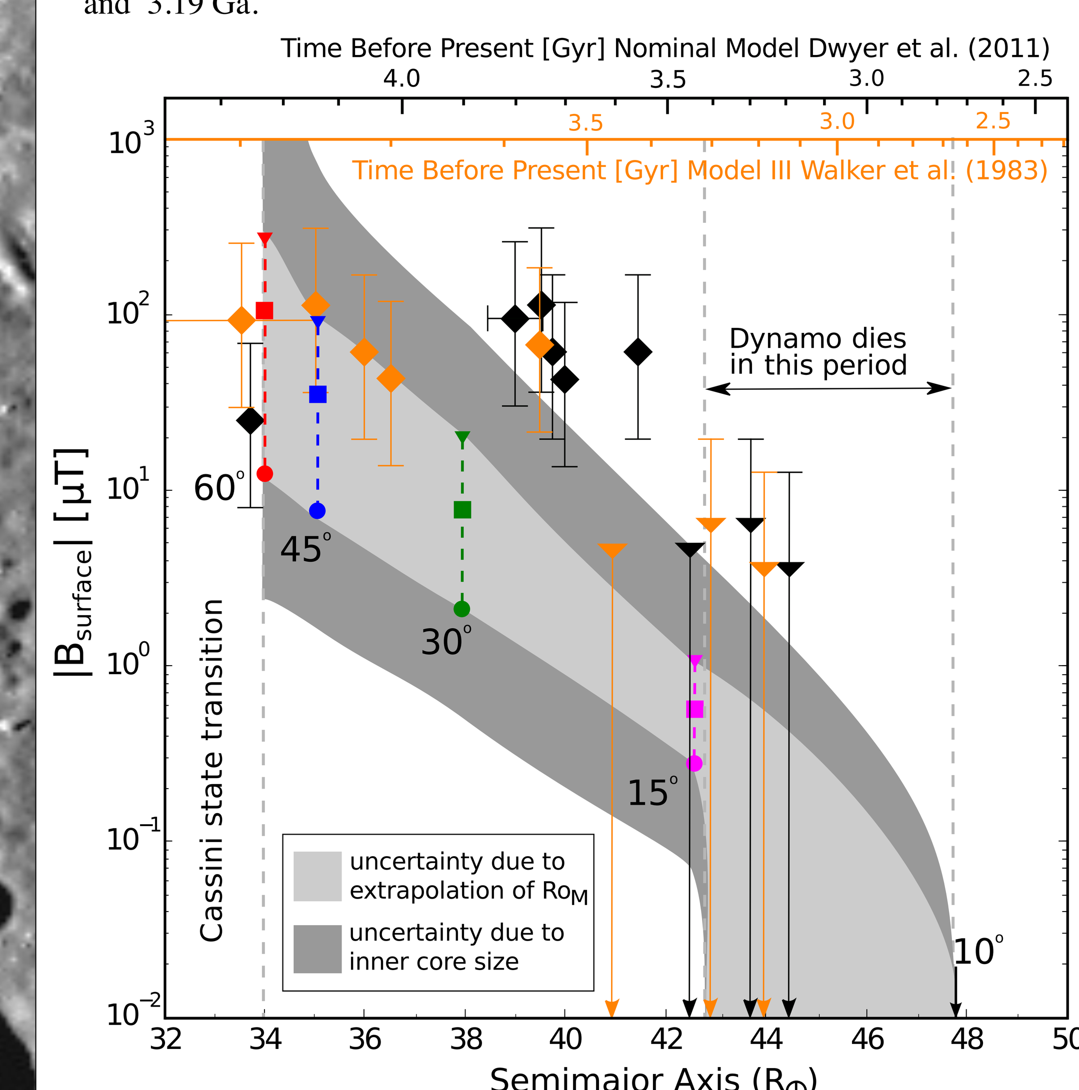

Figure 5. Surface magnetic field intensity vs. lunar semi-major axis using estimates from the magnetic Rossby number scaling study (colours correspond to the colours in Fig. 3). Squares are the extrapolated intensities. Triangles/circles are the upper/lower bounds on modelled surface intensity as explained in Figure 3. Trend lines are drawn to indicate the constraints on the death of the lunar dynamo. Paleointensities obtained from lunar samples are plotted in black and orange depending on the time-axis used [3–6, 14] .

Summary/Conclusions

(1) A mechanically-driven lunar core is capable of dynamo action.

(2) Our model of this type of lunar dynamo produces surface magnetic field strengths in the range of 1 – 100μT after the Cassini transition and before 3.3Ga.

(3) The precessionally driven dynamo naturally dies as the mantle obliquity falls below 10°-15°, consistent with the rapid decline of surface intensities in the paleomagnetic record.

References

[1] M. E. Purucker, J. B. Nicholas, *J. Geophys. Res.* 115, E12007 (2010) [2] C. Cournède, J. Gattacceca, P. Rochette, *Earth Planetary Sci. Lett.*, 331, 31 (2012) [3] I. Garrick-Bethell, B. P. Weiss, D. L. Shuster, J. Buz, *Science,* 323, 356 (2009) [4] E. K. Shea, et al. *Science,* 335, 453 (2012) [5] C. Suavet et al. *PNAS*, 110, 21 (2013) [6] S. M. Tikoo, B. P.Weiss,W. S. Cassata, D. L. Shuster, J. Gattacceca, C. R. Suavet, F. Nimmo, M. D. Fuller, *Earth Planet. Sci. Lett.*, under review (2014) [7] J. S. Halekas, R. P. Lin, D. L. Mitchell, *Meteorit. Planet. Sci.* 38, 565 (2003) [8] L. L. Hood, Icarus 211 (2011) [9] C. A. Dwyer, D. J. Stevenson, F. Nimmo, *Nature*, 479, 212 (2011) [10] J. Meyer, J. Wisdom, *Icarus*, 211, 921 (2011) [11] W. R. Ward, *Science*, 189, 377 (1975) [12] J. G. Williams, D. H. Boggs, C. F. Yoder, J. T. Ratcliff, J. O. Dickey, *Journal of Geophysical Research*, 106, E11 (2001) [13] J. Touma, J. Wisdom, *Astronomical Journal,* 108 (5), 1943 (1994) [14] M. D. Fuller, B. P. Weiss, presented at the 43rd Lunar and Planetary Science Conference, The Woodlands, TX, March 2012 [15] D. J. Webb, *Geophys. J. R. Astron. Soc.* 70, 261 (1982) [16] J. C. G.Walker et al. in Earth's Earliest Biosphere: its origin and evolution (ed. Schopf, J.) 260-290. Princeton Univ. Press, Princeton, NJ. [17] P. Goldreich, *Journal of Geophysical Research*, 72, 12 (1967)